

Brown dwarfs and the cataclysmic variable period minimum

U. Kolb^{1★†} and I. Baraffe²

¹*Astronomy Group, University of Leicester, Leicester LE1 7RH*

²*Ecole Normale Supérieure de Lyon, C.R.A.L. (UMR 5574 CNRS), F-69364 Lyon Cedex 07, France*

Accepted 1999 June 24. Received 1999 June 18; in original form 1999 May 13

ABSTRACT

Using improved, up-to-date stellar input physics tested against observations of low-mass stars and brown dwarfs, we calculate the secular evolution of low-mass donor cataclysmic variables (CVs), including those that form with a brown-dwarf donor. Our models confirm the mismatch between the calculated minimum period ($P_{\min} \approx 70$ min) and the observed short-period cut-off (≈ 80 min) in the CV period histogram. We find that tidal and rotational corrections applied to the one-dimensional stellar structure equations have no significant effect on the period minimum. Theoretical period distributions synthesized from our model sequences always show an accumulation of systems at the minimum period, a feature absent from the observed distribution. We suggest that non-magnetic CVs become unobservable as they are effectively trapped in permanent quiescence before they reach P_{\min} , and that small-number statistics may hide the period spike for magnetic CVs.

Key words: accretion, accretion discs – methods: statistical – binaries: close – stars: evolution – stars: low-mass, brown dwarfs – novae, cataclysmic variables.

1 INTRODUCTION

Cataclysmic variables (CVs) are semi-detached binaries with a white dwarf (WD) primary and a low-mass main-sequence companion that transfers mass to the WD through Roche-lobe overflow (e.g. Warner 1995). Orbital periods are known for about 400 systems. Two marked features stand out in the orbital period distribution: a dearth of systems in the range 2–3 hr, usually referred to as the ‘period gap’, and a sharp short-period cut-off at ≈ 80 min, the ‘period minimum’ P_{\min} (e.g. Ritter & Kolb 1998). J 0132-6554 at $P = 77.8$ min currently marks the short end of the bulk of the distribution, while the single system V485 Cen at $P = 59$ min is the notable exception. Six AM CVn-type CVs with yet shorter periods are interpreted as CVs with helium donors.

In a semi-detached binary, the Roche-lobe filling star’s mean density ρ determines the orbital period P almost uniquely (e.g. King 1988), $P_{\text{h}} = k/\rho_{\odot}^{1/2}$ (where $k \approx 8.85$ is only a weak function of the mass ratio; P_{h} is the period in hours; ρ_{\odot} is the mean density in solar units). The density increases for donors evolving along the hydrogen-burning main sequence towards smaller mass. Approaching the minimum hydrogen-burning mass, the increasing electron degeneracy induces structural changes such that further mass loss reduces ρ . Hence, during the donor’s transition from a main-sequence star to a brown dwarf (BD) the secular mean orbital period derivative changes from negative to positive. This ‘period bounce’ has long been identified with the minimum period

of CVs (Paczynski 1981; Paczynski & Sienkiewicz 1981; Rappaport, Joss & Webbink 1982; D’Antona & Mazzitelli 1982).

The actual period P_{turn} at which a CV bounces depends on the ratio $\tau = t_{\text{KH}}/t_{\text{M}}$ of the secondary’s thermal time $t_{\text{KH}} \sim GM^2/RL$ and mass transfer time $t_{\text{M}} = M/(-\dot{M}_2)$, the characteristic time-scales restoring and perturbing equilibrium. If τ is small, P_{\min} is short. Hence P_{turn} is sensitive both to the orbital angular momentum loss rate (which determines the transfer rate $-\dot{M}_2$) and to the interior structure of the donor. Paczynski (1981) was the first to point out that P_{turn} is close to 80 min if gravitational wave radiation drives the mass transfer. Since then, models with different input physics have been employed to verify a quantitative agreement between the observed P_{\min} and the calculated P_{turn} . Recent calculations (Kolb & Ritter 1992; Howell, Rappaport & Politano 1997) notoriously give P_{turn} too short by typically 10 per cent.

Most of these evolutionary calculations are based on input physics that is rather approximate for very-low-mass (VLM) objects, i.e. donors with mass $\lesssim 1 M_{\odot}$. Because of their relatively high central densities and low central temperatures, correlation effects between particles dominate and must be taken into account in the equation of state (cf. Chabrier & Baraffe 1997, and references therein). Below about $T_{\text{eff}} \approx 4000$ K ($M \lesssim 0.6 M_{\odot}$), molecules become stable and dominate the atmospheric opacity, being responsible for strong non-grey effects and significant departure of the spectral energy distribution from blackbody emission (cf. Allard et al. 1997, and references therein).

Because of significant efforts devoted to the complex physics of low-mass stellar/substellar objects, the theory describing them has improved considerably in the past few years. As a result, the latest

★ Present address: Department of Physics, The Open University, Walton Hall, Milton Keynes, MK7 6AA.

† E-mail: U.C.Kolb@open.ac.uk

generation of stellar models for low-mass stars and brown dwarfs is now able to reproduce observed properties of field M-dwarfs with unprecedented accuracy (cf. Allard et al. 1996; Marley et al. 1996; Chabrier & Baraffe 1997; Burrows et al. 1997; Baraffe et al. 1998).

In this paper we use the Baraffe et al. models (1995, 1997, 1998, henceforth summarized as BCAH) – briefly reviewed in Section 2 – to calculate the secular evolution of CVs in the vicinity of P_{turn} (Section 3.1). We test if tidally distorted stellar models lead to a significant increase of P_{turn} over the value for spherical stars, as claimed by Nelson, Chau & Rosenblum 1985 (Section 3.2), and address the problem of the missing ‘period spike’ at P_{min} (Section 3.3). This predicted accumulation of systems at P_{turn} is caused by the slow velocity in period space close to period bounce, which increases the detection probability. The spike has been a dominant feature in synthesized period distributions obtained from theoretical CV population models (Kolb 1993; Kolb et al. 1998), yet is absent in the observed CV period distribution. In these earlier population models the donor star was approximated as a (bi-)polytrope, and CVs forming with a donor mass smaller than $0.10 M_{\odot}$ were not considered. Here we investigate if the period spike persists in period distributions synthesized from full BCAH models. For the first time, we include CVs that form already with BD donors, i.e. systems that did not evolve through period bounce. In Section 4, alternative explanations for the missing period spike are discussed. In particular, we focus on the difference between magnetic and non-magnetic CVs.

2 INTERNAL STRUCTURE OF THE SECONDARY

Baraffe et al. (1998, and references therein) give a brief account of the input physics used in the most recent low-mass star models we apply here. The main strengths of these models are in two areas: the microphysics determining the equation of state (EOS) in the stellar interior, and the outer boundary condition based on non-grey atmosphere models.

The models employ the Saumon, Chabrier & Van Horn (1995) EOS, which is specifically calculated for VLM stars, BDs and giant planets. The EOS is an important ingredient for our analysis, since it determines the mechanical structure of the donor stars, and thus their *mass–radius relation*. Models based on this EOS have been successfully tested against stars in detached eclipsing binary systems (Chabrier & Baraffe 1995) and field M-dwarfs (cf. Beuermann et al. 1998). The Saumon et al. (1995) EOS has been successfully compared with recent laser-driven shock wave experiments performed at Livermore. These probe the complex regime of pressure dissociation and ionization that is so characteristic for the objects we are studying here (cf. Saumon et al. 1998).

The second important ingredient of our VLM star and BD models concerns the outer boundary condition, which determines the thermal properties of an object and thus the *mass–effective temperature (T_{eff}) relation*. As demonstrated by Chabrier & Baraffe (1997), evolutionary models with a grey atmosphere outer boundary, e.g. the standard Eddington approximation, overestimate T_{eff} for a given mass, and yield too large a minimum hydrogen burning mass (MHBM). Because of tremendous recent progress in the field of cool atmosphere models (see e.g. the review of Allard et al. 1997) these now provide realistic

atmosphere profiles and synthetic spectra, which we use as a more realistic outer boundary condition.

Several observational tests confirm the success of evolutionary models based on these improvements, e.g. mass–magnitude relationships, colour–magnitude diagrams (Baraffe et al. 1997, 1998), mass–spectral type relationships (Baraffe & Chabrier 1996), and the first cool BD, GL 229B (Allard et al. 1996). Although some discrepancies between models and observations remain (see Baraffe et al. 1998), uncertainties attributed to the input physics now seem significantly reduced.

We employ these one-dimensional BCAH models in the context of CVs within the usual Roche approximation. The mass transfer rate is calculated as a function of the difference between donor radius and Roche radius, following Ritter (1988). In a separate set of calculations, we apply tidal and rotational corrections to the one-dimension stellar structure equations (Chan & Chau 1979) to account for the non-spherical shape of Roche equipotential surfaces. This allows us to test the results by Nelson et al. (1985), who found that their distorted stellar models give a value for P_{turn} that is about ≈ 10 per cent longer than for their spherical stellar models.

3 MODEL CALCULATIONS

3.1 Evolutionary sequences

Using the BCAH stellar evolution code we recalculated the secular evolution of short-period CVs for various initial component masses. We assume that orbital angular momentum is lost by gravitational wave emission (e.g. Landau & Lifshitz 1958) and via an isotropic stellar wind from the WD. The wind removes the accreted mass with the WD’s specific orbital angular momentum from the binary. Hence the WD mass is constant throughout the evolution.

As we focus on the period minimum, we do not consider the evolution at periods longer than 2–3 hr. In a second paper (Baraffe & Kolb 1999; see also Kolb & Baraffe 1999) we discuss the properties of such sequences with more massive donors. They depend on the rather uncertain strength of the magnetic braking thought to dominate the evolution of CVs above the period gap (see e.g. King 1988 for a review).

We calculated three sets of evolutionary sequences. In Set A, the WD mass is $0.6 M_{\odot}$, while the initial donor masses range from 0.27 to $0.04 M_{\odot}$ (see Fig. 1). Set B is similar but for a WD mass of $1.0 M_{\odot}$. In Set C, the initial donor mass is fixed at $0.21 M_{\odot}$, while the WD masses range from 1.2 to $0.3 M_{\odot}$; see Table 1. At turn-on of mass transfer, the secondary was either on the ZAMS ($M_2 \geq 0.085 M_{\odot}$), or had an age of 2 Gyr ($M_2 < 0.085 M_{\odot}$). All donors are hydrogen-rich and have solar metallicity ($X = 0.70$, $Z = 0.02$). The sequences were terminated when the donor’s effective temperature T_{eff} was smaller than 900 K. This is the lower limit of the temperature range covered by the present non-grey atmosphere models (Hauschildt, Allard & Baron 1999) available for this study.

Some quantities of interest for a typical sequence starting immediately below the period gap are shown in Fig. 2 and given in Table 2 (see also Table 3 for a sequence initiating mass transfer from a BD donor).

Fig. 1 confirms the well-known effect that systems with different initial donor masses rather quickly join a uniform evolutionary track (Stehle, Ritter & Kolb 1996). Most systems of Set A undergo period bounce at $P_{\text{turn}} \approx 67$ min, which is only

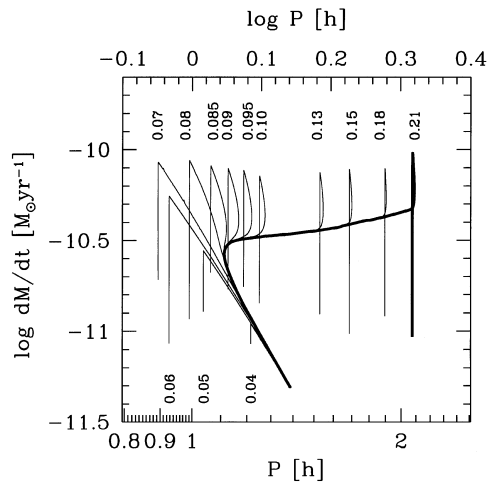


Figure 1. Mass transfer rate versus orbital period for sequences of Set A (white dwarf mass $0.6 M_{\odot}$). Labels indicate the initial donor mass (in units of M_{\odot}).

Table 1. Model parameters of sequences in Set C (initial donor mass $0.21 M_{\odot}$; age of donor at birth of CV 0.61 Gyr). M_1 is the WD mass, t_f the age since formation of the CV when $T_{\text{eff}} = 900$ K, M_{turn} the donor mass at period bounce, \dot{m}_{turn} the transfer rate at period bounce (in $10^{-11} M_{\odot} \text{yr}^{-1}$).

M_1 (M_{\odot})	t_f (Gyr)	P_{turn} (hr)	M_{turn} (M_{\odot})	\dot{m}_{turn}
0.30	8.13	1.068	0.0634	1.94
0.35	7.77	1.078	0.0633	2.11
0.40	7.43	1.087	0.0631	2.21
0.60	6.35	1.113	0.0628	2.65
0.70	5.94	1.123	0.0627	2.84
0.80	5.61	1.133	0.0624	3.03
1.00	5.09	1.149	0.0622	3.36
1.20	4.70	1.162	0.0620	3.64

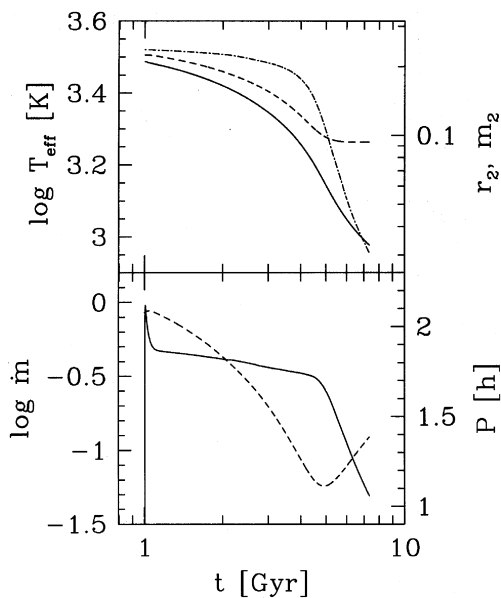


Figure 2. Time evolution of the sequence with $0.6 M_{\odot}$ WD mass, $0.21 M_{\odot}$ initial donor mass sequence. The time t at turn-on of mass transfer has been set arbitrarily to 1 Gyr. *Upper panel:* Effective temperature T_{eff} (dash-dotted; left-hand scale) and radius r_2 (dashed), mass m_2 (solid), both in solar units, right-hand scale, of the donor. *Lower panel:* Mass transfer rate \dot{m} (in $10^{-10} M_{\odot} \text{yr}^{-1}$; solid) and orbital period P (dashed).

Table 2. Characteristic quantities along the sequence with initial donor mass $0.21 M_{\odot}$ and WD mass $0.6 M_{\odot}$. t is the age in gigayears, P_h the orbital period in hours; M the donor mass in units of M_{\odot} ; T_{eff} the effective temperature in kelvins; L corresponds to $\log L/L_{\odot}$; R is the radius in solar units, and \dot{M} the transfer rate in units of $M_{\odot} \text{yr}^{-1}$.

t (Gyr)	P_h	M	T_{eff}	L	R/R_{\odot}	$\log \dot{M}$
0.00	2.080	0.2103	3311.	-2.272	0.2242	-16.00
0.25	2.038	0.1975	3288.	-2.313	0.2168	-10.34
0.50	1.970	0.1862	3264.	-2.363	0.2077	-10.35
0.75	1.902	0.1753	3239.	-2.415	0.1987	-10.37
1.00	1.832	0.1648	3212.	-2.470	0.1898	-10.38
1.25	1.764	0.1545	3177.	-2.530	0.1810	-10.39
1.50	1.696	0.1446	3133.	-2.596	0.1725	-10.41
1.75	1.628	0.1351	3087.	-2.665	0.1640	-10.43
2.00	1.556	0.1259	3044.	-2.736	0.1554	-10.44
2.25	1.483	0.1169	2993.	-2.815	0.1469	-10.45
2.50	1.409	0.1082	2929.	-2.904	0.1384	-10.46
2.75	1.336	0.0996	2849.	-3.007	0.1300	-10.47
3.00	1.265	0.0912	2743.	-3.129	0.1217	-10.48
3.25	1.200	0.0830	2607.	-3.275	0.1140	-10.49
3.50	1.148	0.0750	2423.	-3.456	0.1071	-10.50
3.75	1.119	0.0675	2205.	-3.665	0.1017	-10.54
4.00	1.114	0.0607	1972.	-3.890	0.0980	-10.60
4.25	1.130	0.0549	1750.	-4.117	0.0958	-10.68
4.50	1.157	0.0501	1570.	-4.317	0.0946	-10.77
4.75	1.189	0.0463	1417.	-4.503	0.0939	-10.86
5.00	1.223	0.0432	1280.	-4.682	0.0935	-10.94
5.25	1.257	0.0406	1176.	-4.830	0.0934	-11.02
5.50	1.290	0.0384	1091.	-4.961	0.0934	-11.10
5.75	1.321	0.0365	1025.	-5.070	0.0934	-11.17
6.00	1.350	0.0350	968.	-5.168	0.0934	-11.23
6.25	1.377	0.0336	918.	-5.260	0.0934	-11.29
6.35	1.387	0.0331	900.	-5.295	0.0935	-11.31

Table 3. Same as Table 2, but for a BD CV sequence with initial donor mass $M_2 = 0.07 M_{\odot}$ and WD mass $0.6 M_{\odot}$.

t (Gyr)	P_h	M	T_{eff}	L	R/R_{\odot}	$\log \dot{M}$
0.00	0.895	0.0700	1796.	-4.141	0.0887	-16.00
0.25	1.041	0.0571	1626.	-4.282	0.0919	-10.47
0.50	1.118	0.0505	1475.	-4.444	0.0927	-10.68
0.75	1.172	0.0461	1334.	-4.617	0.0929	-10.82
1.00	1.218	0.0428	1220.	-4.770	0.0931	-10.93
1.25	1.259	0.0402	1129.	-4.904	0.0932	-11.02
1.50	1.295	0.0380	1056.	-5.019	0.0933	-11.11
1.75	1.328	0.0362	994.	-5.122	0.0934	-11.18
2.00	1.358	0.0347	943.	-5.214	0.0935	-11.24
2.01	1.359	0.0346	940.	-5.219	0.0935	-11.24

slightly longer than the corresponding $P_{\text{turn}} = 65$ min found with Mazzitelli's models (Kolb & Ritter 1992; see also the dotted curve in Fig. 3, lower panel). Note that a grey outer boundary condition like the standard Eddington approximation yields a smaller radius for given donor mass $M_2 \leq 0.2 M_{\odot}$, and a higher MHB. A test calculation with fixed mass loss rate and the Eddington approximation gives P_{turn} shorter by 5 min than for the corresponding sequence based on non-grey atmosphere models. Note also that CVs forming with fairly old and massive brown-dwarf donors (age ≥ 2 Gyr, mass 0.05 – $0.07 M_{\odot}$) would populate the period regime shortwards of P_{turn} . V485 Cen might be such a system.

For Set B, we have $P_{\text{turn}} = 69$ min, slightly longer than for Set A since gravitational radiation losses are higher for larger WD mass, hence the mass transfer rate is larger. The dependence of P_{turn} on WD mass is most easily seen in Fig. 3, upper panel.

The effective temperature of the donor as a function of period is

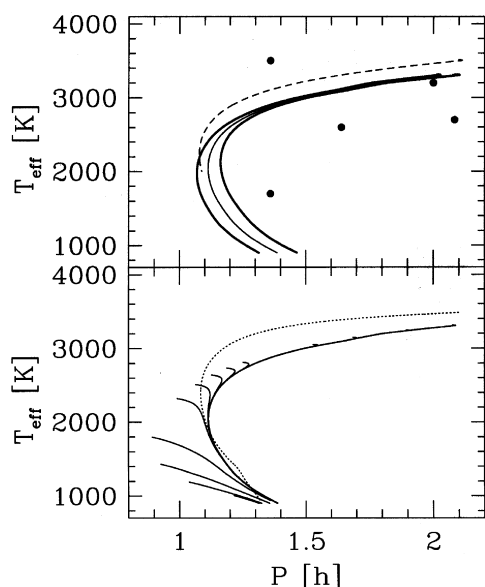


Figure 3. Effective temperature versus orbital period for various evolutionary sequences. *Upper panel:* Sequences with different WD masses. Solid: 1.2, 0.6, 0.3 M_{\odot} , in order of decreasing P_{turn} . Dashed: 0.70 M_{\odot} , but with a low-metallicity donor ($Z = 0.006$). Dots show the claimed location of AL Com (Howell, Hauschildt & Dhillon 1998), WZ Sge, TY Psc, V592 Cas, and HU Aqr (Ciardi et al. 1998). *Lower panel:* Sequences (of Set A) with different initial donor masses (solid; see also Fig. 1). Dotted: a 0.7 M_{\odot} WD mass sequence, calculated with Mazzitelli's (1989) stellar evolution code.

shown in Fig. 3. The asymptotic convergence of sequences with different initial donor mass and the insensitivity of \dot{M} to the WD mass result in an essentially unique relation $T_{\text{eff}}(P)$ on the non-degenerate branch of the track (before period bounce occurs). At P_{turn} , and on the degenerate branch (after period bounce) there is a significant spread in T_{eff} for given P . In the same diagram, dots indicate the claimed location of AL Com (Howell et al. 1998), WZ Sge, TY Psc, V592 Cas and HU Aqr (Ciardi et al. 1998). For these systems, the effective temperature of the donor has been derived via spectral fittings in the near-infrared using the same atmosphere models (Hauschildt et al. 1999) that serve as the outer boundary condition of our stellar models. Since the near-IR emission of CVs is produced by both the secondary and the accretion disc, the estimate of the secondary's contribution may be rather uncertain because of the lack of reliable accretion disc models. We thus do not regard the discrepancy between model calculations and observational data points (cf. Fig. 2) as significant.

3.2 Sequences with non-spherical donors

We implemented the rotational correction scheme of Chan & Chau (1979) to investigate the effect of rotation and tidal distortion on the donor star. Assuming solid-body rotation, we recalculated a sequence with 0.21 M_{\odot} initial donor mass, 1.0 M_{\odot} WD mass and $\dot{J} = \dot{J}_{\text{GR}}$. We find that P_{turn} is hardly affected; it is longer by only 1 min compared to the corresponding sequence with spherical models (from Set B). We have performed several other experiments, with different initial secondary masses and mass transfer rates (constant, or as given by gravitational radiation), including the case considered by Nelson et al. (1985), i.e. $M_1 = 1.0 M_{\odot}$, $M_2 = 0.4 M_{\odot}$, $\dot{J} = \dot{J}_{\text{GR}}$. In none of these sequences could we reproduce the significant effect (~ 10 per cent) rotational and tidal corrections had on P_{turn} in

the calculations by Nelson et al. (1985) based on the same scheme of Chan and Chau (1979).

We do not think that the discrepancy between Nelson et al. (1985) and our work results from differences in the EOS and opacities. Indeed, although our input physics differs from those adopted by Chan & Chau (1979), we find the same quantitative differences quoted by these authors between the properties (L , R and T_{eff}) of spherical and rotating ZAMS stars (cf. their table 1). We also reproduce the effects quoted in the very recent paper by Sills & Pinsonneault (1999). They considered a 0.7 M_{\odot} ZAMS star with equatorial rotational velocity 145 km s^{-1} and found a slightly increased surface luminosity and effective temperature ($\Delta \log L = 3.2$ per cent, $\Delta T_{\text{eff}} = 100$ K) compared to non-rotating models. For the same case we find $\Delta \log L = 4.5$ per cent, $\Delta T_{\text{eff}} = 90$ K.

We are thus confident in our results and conclude that rotational and tidal corrections as described by Chan and Chau (1979) can be neglected for CVs, even when the systems are close to period bounce. Note that, although the secondary spins up in evolving toward P_{turn} , the key quantity defined by Chan and Chau (1979),

$$\alpha = \frac{2 \omega^2 R^3}{3 GM_{\text{R}}},$$

which appears in the momentum equation and represents the ratio of rotational to gravitational potential gradient, remains essentially constant at the donor star surface during the evolution (recall that the angular velocity $\omega^2 \propto P^{-2} \propto M_2/R_2^3$). The maximum value of α , reached at the surface, never exceeds 0.07.

Given the small differences between spherical and tidally distorted models, we use the less cpu-time intensive calculations with spherical stars to derive a period distribution and analyse its properties close to P_{min} .

3.3 Generating a period histogram

When the evolutionary sequences presented in Section 3.1 are convolved with an appropriate CV formation rate they give a theoretically predicted period histogram in the vicinity of P_{min} (see Kolb 1993 for a detailed description of the population synthesis technique). De Kool (1992) and Politano (1996) calculated the formation of CVs with standard assumptions about common envelope evolution and magnetic braking (see e.g. Kolb 1996 for a review). We computed population models for all these formation rate models; in addition, to show the differential effect of the main parameters more clearly, we considered subpopulations for a given WD mass with a time-independent formation rate $b(\log M_2) = \text{const.}$ in certain $\log M_2$ intervals.

In Figs 4 and 5 we show period distributions for two different CV subpopulations – P1 and P2 – which allow one to study the main effects that determine the structure of the histogram at P_{min} . The histograms are for either a volume-limited sample, or a sample where individual systems have been weighted by \dot{M}^{α} , for various values of α . This mimics selection effects which affect the observed sample (cf. Kolb 1996). The subpopulations formally correspond to a galactic disc age of 6 Gyr. In a somewhat older population, the edge of the volume-limited distributions at ≈ 1.4 hr would appear at slightly longer P , while the \dot{M}^{α} -weighted cases would hardly change.

P1. Period histograms obtained from Set A (Fig. 4). These correspond to the period distribution of a subset of CVs with WD mass 0.6 M_{\odot} (assuming that this mass does not change through the

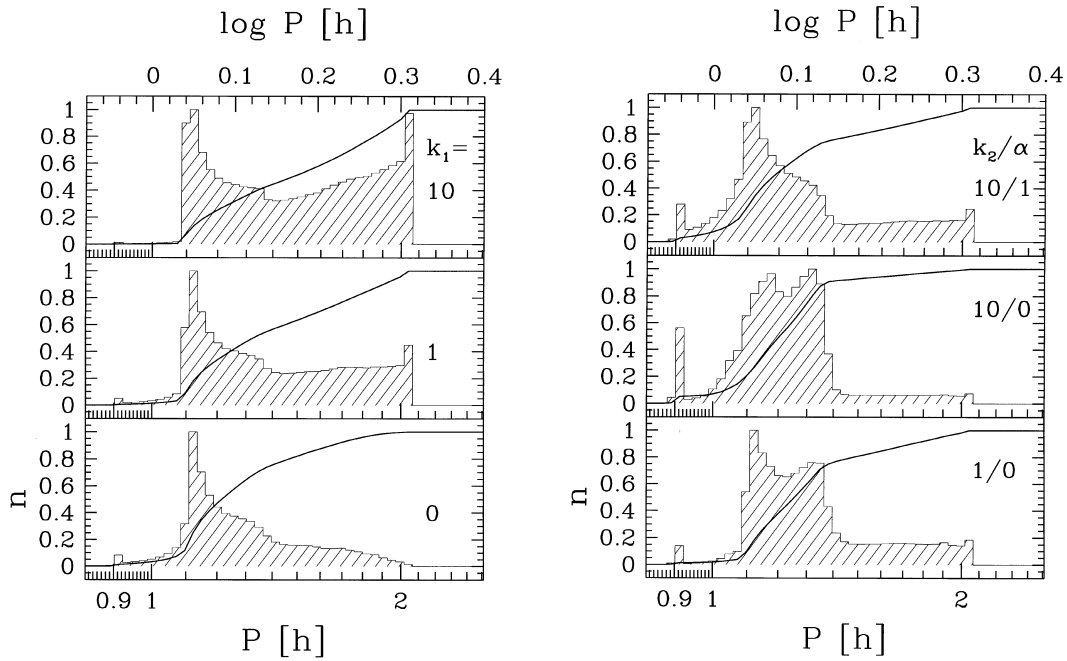


Figure 4. Orbital period distributions $n(\log P)$ for CVs with a $0.6 M_{\odot}$ WD, synthesized from Set A and formation rate (1), arbitrarily normalized, for different fractions k_1 of systems forming above the period gap, fractions k_2 of CVs forming with BD donors, and detectability parameters α (see text for details). The solid curves are the corresponding cumulative distributions $N(> P)$. *Left:* $k_2 = 1$, $\alpha = 1$ in all models, k_1 as labelled. *Right:* $k_1 = 1$ in all models, k_2 and α as labelled.

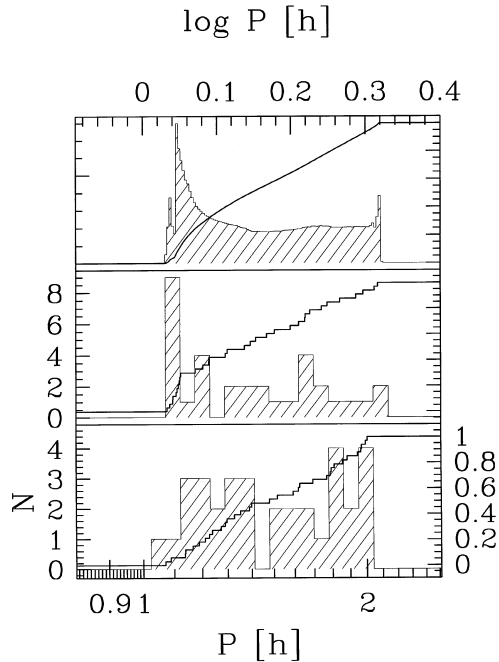


Figure 5. *Upper panel:* synthesized orbital period distribution P2 (see text), for $\alpha = 1.5$. *Middle and lower panels:* two arbitrary samples of 33 systems drawn from the distribution in the upper panel.

evolution). The same analysis has been performed for sequences of Set B, with very similar results, which we therefore do not show.

As noted above we do not consider the evolution of CVs with donors $> 0.21 M_{\odot}$, i.e. of CVs that form above the period gap. In the disrupted magnetic braking model for the period gap (e.g.

King 1988) these systems would all reappear $\lesssim 10^8$ yr after formation at the lower edge of the gap, with a donor in thermal equilibrium. A BCAH stellar model in thermal equilibrium with mass $\approx 0.21 M_{\odot}$ would fill its Roche lobe at $P = 2.1$ hr, the observed lower edge of the period gap. Hence we simulate the contribution of systems that form above the gap to the period distribution below the gap by increasing the formation rate in a narrow bin in M_2 -space at $0.21 M_{\odot}$ by a large factor.

For the first time, we explicitly include systems that form with a brown-dwarf donor star. The formation rate of such BD CVs is not known. Survival of the common envelope phase is crucial and could be a problem as the maximum orbital energy available to eject the envelope, roughly $\propto M_2$, is small. Simulations by Politano (private communication) show that the formation of BD CVs is possible when the same formalism is applied as for more massive donor stars. For our purposes we just extrapolate the birthrate function $b_2(\log M_2)$ down to the smallest initial donor mass ($0.04 M_{\odot}$) considered here.

In particular, we use

$$b_2(\log M_2) = \begin{cases} 0.368k_1, & 0.207 \leq M_2/M_{\odot} < 0.210 \\ 1, & 0.090 < M_2/M_{\odot} \leq 0.207 \\ k_2, & 0.040 \leq M_2/M_{\odot} \leq 0.090 \end{cases} \quad (1)$$

with various combinations of the free parameters k_1 and k_2 , describing the relative weight of systems forming above the period gap and with a brown-dwarf donor, respectively. The numerical factor in front of k_1 is chosen such that for $k_1 = 1$ as many CVs form with donor masses $0.21 < M_2/M_{\odot} \leq 1.0$ (‘above the gap’) as with masses $0.09 \leq M_2/M_{\odot} \leq 0.21$ (‘below the gap’). The results are not sensitive to the choice of the boundaries at 0.207 and $0.09 M_{\odot}$. So, chiefly, k_1 is the ratio of systems forming above the gap to systems forming below the gap with a non-degenerate

donor, while k_2 is the ratio of the formation rate of CVs with degenerate and non-degenerate donors. Fig. 4 shows period histograms for various combinations of k_1 , k_2 and α .

P2. A period histogram obtained from Set C, with the full time-dependent formation rate calculated by de Kool (1992; his model 3). This distribution, shown in the top panel of Fig. 5, illustrates the fine structure of the period spike at P_{turn} as a result of the different WD masses in the sample. To obtain this histogram, we approximated sequences with an arbitrary initial donor mass $M_2 < 0.21 M_\odot$ by the $0.21 M_\odot$ sequence from M_2 onwards. This introduces a slight error at the onset of mass transfer and for sequences that would form close to P_{turn} . An explicit comparison of results from this simplified method for $0.6 M_\odot$ WD mass with the distribution obtained from the full set of sequences (Set A) shows that these deviations are negligible as long as $k_2 \lesssim 2$. To estimate the contribution from systems that form above the period gap, the actually calculated evolutionary tracks have been extended to donor masses $> 0.21 M_\odot$ by assuming a simple main-sequence mass–radius relation (such that $P \propto M_2$) and a constant mass-transfer rate ($2 \times 10^{-9} M_\odot \text{ yr}^{-1}$).

The theoretical period distributions in Figs 4 and 5 show that the collective period minimum P_{min} coincides with the bounce period P_{turn} of individual evolutionary sequences, and is about 10 min shorter than the observed period minimum (e.g. Ritter & Kolb 1998). This confirms tentative conclusions reached earlier by Kolb (1993), who considered populations constructed from simplified polytropic stellar models with artificial outer boundary conditions, and restricted to initial donor masses $\geq 0.09 M_\odot$.

The subpopulations for WD masses of 0.6 and $1.0 M_\odot$ show that the period spike does not disappear or broaden significantly when CVs with brown-dwarf donor stars are included in the population. This is true unless the majority of newly forming CVs actually are BD CVs ($k_2 \gtrsim 5$). But if BD CVs were dominant, the bulk of systems would populate the period regime shortwards of P_{turn} , making this a fairly unlikely possibility in view of the observed value of P_{min} .

In fact, in population models that do not explicitly over-emphasize BD CVs ($k_2 \lesssim 2$) the effect of these sequences on the overall shape of the period spike is generally small. A fair representation of the period spike is obtained by the simple procedure used to generate the period distribution P2. The double spike at P_{min} in the P2 histogram (Fig. 5, upper panel) is a result of the double-humped WD mass distribution (see e.g. de Kool 1992): high-mass C/O WD systems cluster in the longer-period spike, low-mass He–WD systems in the shorter-period spike. This fine structure of course disappears altogether in small samples.

The overall shape of the weighted distribution is not sensitive to moderate α ; there is hardly any difference between histograms calculated with α between 0.5 and 1.5. Increasing α further tends to decrease the amplitude of the spike. We obtain a truly flat distribution, similar to the observed one (Fig. 6), only for $\alpha \gtrsim 6$.

4 DISCUSSION

The results presented in the previous section show that despite the significant improvement of low-mass star and brown-dwarf models, the period histogram for short-period CVs synthesized from these models still appears to be in conflict with observations. If the evolution of short-period CVs is driven by the emission of gravitational waves, period bounce occurs at ≈ 70 min for most

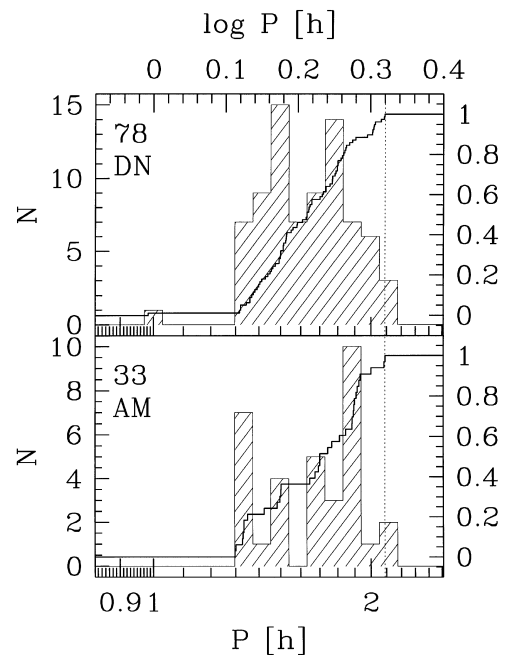


Figure 6. The observed orbital period distribution of dwarf novae (upper panel) and polars (lower panel), for systems with $P_h < 2.1$. The solid curve is the normalized cumulative distribution. Data from Ritter & Kolb (1998).

systems, resulting in a collective minimum period P_{min} that is 10 min shorter than the observed one. The contribution of CVs forming with BD donors is either negligible or would cause P_{min} to be yet shorter. As a result of period bounce, the simulated period histograms show an accumulation of systems near P_{min} , the period spike. The only way to remove the period spike effectively from the distribution is to impose a very steep dependence of the system’s detectability d on one of the evolutionary parameters, e.g. $\propto \dot{M}^6$ or steeper.

The catalogue of Ritter & Kolb (1998) lists 129 CVs with periods < 2.10 hr. Among these are 33 polars, 78 dwarf novae (excluding intermediate polars), and 6 AM CVn systems. The remaining 12 systems are either intermediate polars, novae, novalikes, or of unknown type. Hence essentially all known short-period CVs are either dwarf novae, i.e. systems with an unstable accretion disc, or discless polars.

4.1 The missing period spike

Almost all dwarf novae are detected in outburst. It is tempting to identify the accretion disc and its outburst properties as the cause for a strong \dot{M} -dependent selection effect. A few short-period dwarf novae, sometimes referred to as WZ Sge stars, have very long outburst recurrence times t_{rec} , the most extreme example being WZ Sge itself with $t_{\text{rec}} \approx 30$ yr. It has long been noted that low- \dot{M} CVs might have escaped detection if their outburst interval were significantly longer than the period since the beginning of systematic monitoring and surveying of the sky by modern means – a few decades. For long t_{rec} , the relative detection probability of dwarf novae scales as $d \propto 1/t_{\text{rec}}$, suggesting that $t_{\text{rec}} \propto \dot{M}^{-6}$ or steeper. In practice this very steep dependence would require that $t_{\text{rec}} \rightarrow \infty$ for $\dot{M} \lesssim \text{few} \times 10^{-11} M_\odot \text{ yr}^{-1}$, i.e. low- \dot{M} CVs would not undergo outbursts at all.

Various plausible physical models that naturally account for this

property have been suggested. Evaporation of accreted material into a hot corona could prevent the disc from accumulating the critical surface mass density required to launch a heating wave (Meyer-Hofmeister, Meyer & Liu 1998; see also Liu, Meyer & Meyer-Hofmeister 1997). Systems in such a permanent quiescence would be optically very faint but should still emit about 10 per cent of their accretion luminosity $L_{\text{acc}} = GM_1\dot{M}/R_1$ (M_1 and R_1 are the WD's mass and radius) in X-rays. Alternatively, King (1999) argues that systems approaching the period minimum become magnetic ejectors even if the WD's magnetic field is weak. In this case an accretion disc can no longer form, and the systems become unobservable. WZ Sge, where the WD is suspected to be weakly magnetic (see e.g. Lasota, Kuulkers & Charles 1999 and references therein), would be a marginal disc accretor (Wynn & Leach 1999).

Although this can explain the absence of a period spike at P_{min} for dwarf novae, it certainly does not apply to the discless polars. An independent observational selection effect operating on polars in the same period/mass transfer rate range and with the same net result as a steep increase of t_{rec} for dwarf novae seems a highly unlikely coincidence (but see Meyer & Meyer-Hofmeister 1999). In other words: polars should show a period spike, even though dwarf novae do not. Could small-number statistics hide the period spike for polars? To investigate this we performed a number of Monte Carlo experiments, where we drew a sample of either 33 or 78 systems from an underlying period distribution like the one shown in Fig. 5 (upper panel). As the middle and lower panels of this figure show, the smaller samples give a surprisingly wide variety of distributions, with typically 20–25 per cent of them showing no sign of a period spike at all. In contrast, in the larger sample the spike is prominent in more than 90 per cent of all cases. A KS test confirms this impression: We wish to quantify the difference between model and observed distribution that is due to a different morphological shape. Therefore we have to exclude effects arising from different values for the lower edge P_{gap} of the period gap and for P_{min} – the latter effect is considered in Section 4.2. To achieve this we rescale the calculated distribution such that it matches the range of the observed distribution before performing the KS test. Specifically, the period axis $C = \log P$ of the theoretical distribution is rescaled according to

$$C \mapsto (C - O_l) \times \frac{O_u - O_l}{C_u - C_l} + O_l, \quad (2)$$

where $C_l = \log P_{\text{min}}$, $C_u = \log P_{\text{gap}}$ denote the calculated period minimum and lower edge of the gap, and O_l , O_u the corresponding observed values. We applied (2) to the model distribution shown in Fig. 5 ($P_{\text{min}} = 64$ min, $P_{\text{gap}} = 124$ min), assuming the observed values $P_{\text{min}} = 78$ min, $P_{\text{gap}} = 113$ min. The maximum significance level for rejecting the null hypothesis that the observed sample is drawn from this rescaled model distribution is 0.34 for polars, 0.98 for dwarf novae. If we use $P_{\text{gap}} = 130$ min for the observed lower edge of the gap, the rejection significance for polars rises to 0.91. This is solely due to the so-called ‘114 min spike’, see e.g. Ritter & Kolb 1992, still a significant feature in the observed distribution.

4.2 The mismatch between observed and calculated P_{min}

Neither the small-number statistics for polars nor the suggested detectability function for dwarf nova can make the minimum period of the observed distribution significantly longer than in the

underlying intrinsic distribution. To achieve this by the latter effect, dwarf novae have to become unobservable long *before* they reach P_{turn} . With \dot{M} as the most likely control parameter determining the detectability this is difficult to achieve, as \dot{M} is almost constant on the non-degenerate branch above P_{turn} . (This problem would be less severe if the main control parameter were the donor mass, the mass ratio, or the orbital separation. A particularly steep dependence of the discovery probability on any of these could be realized if mass transfer cycles, similar to the ones discussed by King et al. 1996, 1997, existed in CVs below the period gap, but changed their character discontinuously before P_{turn} .)

To test the effect of small-number statistics we drew 1000 samples of either 33 or 78 systems from the theoretical distribution shown in Fig. 5 and registered the shortest period P_s of each sample. The parent distribution has a short-period cut-off at 64.4 min. We found that 99.9 per cent of the larger samples have $P_s < 67.0$ min (99.0 per cent have $P_s < 66.6$ min, 90.0 per cent have $P_s < 65.6$ min). The median is $P_s = 65$ min, the longest P_s we found is 67.03 min. Similarly, 99.9 per cent of the smaller samples have $P_s < 71.0$ min (99.0 per cent have $P_s < 68.2$ min, 90.0 per cent have $P_s < 66.8$ min), with a median $P_s = 65.4$ min, and 71.2 min as the longest P_s . The rare cases where P_s was as long as 70 min still fall well short of the observed value $P_{\text{min}} = 78$ min.

Given this, it might be that the P_{min} mismatch is caused by evolutionary effects after all – effects not accounted for in our models.

The chemical composition of the secondary affects the value of P_{turn} , by changing the parameter of the donor at a given mass, hence changing both t_M (via the angular momentum loss time) and t_{KH} . Stehle, Kolb & Ritter (1997) pointed out that P_{turn} is slightly shorter for CVs with low-metallicity donors. They found $dP_{\text{turn}}/d \log Z = 0.084$ hr. Our calculations confirm this ($P_{\text{turn}} = 67.41$ min for $Z = 0.02$, while $P_{\text{turn}} = 64.70$ min for $Z = 0.006$; both with $M_1 = 0.70 M_{\odot}$). Although P_{turn} increases for higher metallicity donors, the effect is much too small to account for a mismatch of 10 min. It has been noted that a larger than expected fraction of CVs above the gap have a nuclear-evolved secondary (Beuermann et al. 1998, Baraffe & Kolb 1999, Kolb & Baraffe 1999). When these secondaries become fully convective their helium content is ~ 0.5 , giving a P_{turn} that is in fact ≈ 7 min *shorter* than for hydrogen-rich donors.

Residual shortcomings in the EOS and the atmosphere profiles cannot yet be ruled out as the cause for the P_{min} discrepancy. A quantitative estimate of uncertainties in the mass–radius relation from the treatment of the EOS (see Saumon et al. 1995) is difficult. The most profound observational test is against stellar parameters determined for components in (detached) eclipsing binaries; yet to date there are no such systems with $M_2 < 0.2 M_{\odot}$. The region near P_{turn} involves effective temperatures lower than 2600 K (cf. Fig. 3), below which grains form. These affect both the atmosphere spectrum and profile. Although the atmosphere models used for this study are grainless, calculations based on preliminary atmosphere models including the formation and absorption of grains (Allard 1999; Baraffe & Chabrier 1999) do not yield a longer P_{turn} . We thus do not expect an improvement of the situation with the forthcoming generation of dusty atmosphere models.

The P_{min} mismatch could also be due to uncertainties in the calculated value of P_{turn} inherent in the very concept of the Roche model. Strictly valid only for point masses, its applicability to extended donors relies on the fact that the stars are usually sufficiently centrally condensed. This is not necessarily a good

approximation for fully convective stars that are essentially polytropes of index $n = 3/2$. We note that Uryu & Eriguchi (1999) considered stationary configurations of fluids describing a synchronously rotating polytropic star in a binary with a point mass companion. For $n = 3/2$ polytropes they find a Roche radius that is typically 1–2 per cent smaller than estimated from Eggleton's (1983) approximation for a given orbital separation, but at the same time ≈ 4 per cent larger than the radius of a non-rotating polytrope with the same mass.

Alternatively, an obvious way to increase P_{\min} is to increase the orbital angular momentum loss rate \dot{J} over the value \dot{J}_{GR} set by gravitational radiation. We find $P_{\min} \approx 83$ min (up from 69 min) for $\dot{J} = 4 \times \dot{J}_{\text{GR}}$ and $M_1 = 1 M_{\odot}$, a much smaller increase than quoted by Paczyński (1981). Patterson (1998) favoured a modest increase of \dot{J} on grounds of space density considerations and the ratio of systems below and above the period gap. Standard population models typically give a local CV space density of up to 10^{-4} pc^{-3} (de Kool 1992; Kolb 1993; Politano 1996), with 99 per cent of all CVs below the period gap, 70 per cent of these past period bounce. Patterson argues that the observed space density is at least a factor 20 smaller, and that there is little evidence for the predicted large population of post-period minimum CVs. A higher transfer rate after period bounce would remove systems from the population as the donor can lose all its mass in the age of the galaxy, thus resolving both problems and the P_{\min} mismatch. However, postulating an as yet unknown \dot{J} mechanism that conspires to produce almost the same value as \dot{J}_{GR} at the transition from non-degenerate to degenerate stars does not seem very attractive. Rather, it seems more likely that the bulk of short-period systems are indeed unobservable – at least in the optical. Watson (1999) shows that the presence of a population of CVs with a space density of 10^{-4} pc^{-3} that emits 10 per cent of its accretion luminosity as X-rays cannot be excluded from *ROSAT* and *ASCA* data. It should be possible to place tight limits on such a population and its potential contribution to the Galactic Ridge emission from deep *XMM* and *AXAF* surveys.

As a final note, we point out that the evolutionary effect of an irradiation-induced stellar wind from the donor (considered semi-analytically by King & van Teeseling 1998) could help to resolve the P_{\min} mismatch and the period spike problem; detailed investigations are under way (Kolb et al. in preparation).

5 SUMMARY

We have investigated the problem that the standard explanation for the CV period minimum as a result of period bounce of systems driven by gravitational radiation predicts a period minimum that is too short, and an accumulation of systems close to P_{turn} , the 'period spike', that is not observed.

Using up-to-date stellar models by Baraffe et al. (1998), which successfully reproduce observed properties of single low-mass stars and brown dwarfs, we confirm that P_{turn} is about 10 min shorter than the observed P_{\min} .

We have presented synthesized period histograms for CVs below the period gap which, for the first time, are based on evolutionary calculations obtained with full stellar models, and include CVs that form with brown-dwarf donors. The period spike is always present.

Although there are ways to explain why the spike is not observed – small-number statistics for polars, undetectability for

dwarf novae – we find no satisfactory reason for the fact that P_{\min} is longer than P_{turn} for both magnetic and non-magnetic CVs.

ACKNOWLEDGMENTS

We are grateful to H. Ritter, H. Spruit, F. Meyer, E. Meyer-Hofmeister and K. Beuermann for valuable discussions, and A. King for comments and for improving the language of the manuscript. We thank the referee T. Marsh for useful comments. IB thanks the Max-Planck-Institut für Astrophysik and the University of Leicester for hospitality during the realization of part of this work. The calculations were performed on the T3E at Centre d'Etudes Nucléaires de Grenoble.

REFERENCES

- Allard F., 1999, in *Very Low-Mass Stars and Brown Dwarfs in Stellar Clusters and Associations*, Euroconference, La Palma, 1998
- Allard F., Hauschildt P. H., Baraffe I., Chabrier G., 1996, *ApJ*, 465, L123
- Allard F., Hauschildt P. H., Alexander D. R., Starrfield S., 1997, *ARA&A*, 35, 137
- Baraffe I., Chabrier G., 1996, *ApJ*, 461, L51
- Baraffe I., Chabrier G., 1999, in *Very Low-Mass Stars and Brown Dwarfs in Stellar Clusters and Associations*, Euroconf., La Palma, 1998
- Baraffe I., Chabrier G., Allard F., Hauschildt P. H., 1995, *ApJ*, 446, L35
- Baraffe I., Chabrier G., Allard F., Hauschildt P. H., 1997, *A&A*, 327, 1054
- Baraffe I., Chabrier G., Allard F., Hauschildt P. H., 1998, *A&A*, 337, 403
- Beuermann K., Baraffe I., Kolb U., Weichhold M., 1998, *A&A*, 339, 518
- Burrows A. et al., 1997, *ApJ*, 491, 856
- Chabrier G., Baraffe I., 1995, *ApJ*, 451, L29
- Chabrier G., Baraffe I., 1997, *A&A*, 327, 1039
- Chan K. L., Chau W. Y., 1979, *ApJ*, 233, 950
- Ciardi D. R., Howell S. B., Hauschildt P. H., Allard F., 1998, *ApJ*, 504, 450
- Clemens J. C., Reid I. N., Gizis J. E., O'Brien M. S., 1998, *ApJ*, 496, 392
- D'Antona F., Mazzitelli I., 1982, *ApJ*, 260, 722
- de Kool M., 1992, *A&A*, 261, 188
- Eggleton P. P., 1983, *ApJ*, 268, 368
- Hauschildt P. H., Allard F., Baron E., 1999, *ApJ*, 512, 377
- Howell S. B., Rappaport S., Politano M., 1997, *MNRAS*, 287, 929
- Howell S. B., Hauschildt P., Dhillion V. S., 1998, *ApJ*, 494, L224
- King A. R., 1988, *QJRAS*, 29, 1
- King A. R., 1999, in Charles P. A., King A. R., O'Donoghue D., eds, *Cataclysmic Variables: a 60th Birthday Symposium in Honour of Brian Warner*. New Astronomy Reviews, in press
- King A. R., van Teeseling A., 1998, *A&A*, 338, 965
- King A. R., Frank J., Kolb U., Ritter H., 1996, *ApJ*, 467, 761
- King A. R., Frank J., Kolb U., Ritter H., 1997, *ApJ*, 482, 919
- Kolb U., 1993, *A&A*, 271, 149
- Kolb U., 1996, in Evans A., Wood J. H., eds, *Cataclysmic Variables and Related Objects*. Kluwer, Dordrecht, IAU Coll. 158, p. 433
- Kolb U., Baraffe I., 1999, in Hellier C., Mukai K., eds, *ASP Conf. Ser. Vol. 197, Annapolis Workshop on Magnetic Cataclysmic Variables*, p. 273
- Kolb U., Ritter H., 1992, *A&A*, 254, 213
- Kolb U., King A. R., Ritter H., 1998, *MNRAS*, 298, L29
- Landau L., Lifshitz E., 1958, *Classical Theory of Fields*, Pergamon, Elmsford
- Lasota J. P., Kuulkers E., Charles P., 1999, *MNRAS*, in press (astro-ph/9901295)
- Liu B. F., Meyer F., Meyer-Hofmeister E., 1997, *A&A*, 328, 247
- Marley M. S., Saumon D., Guillot T., Freedman R., Hubbard W. B., Burrows A., Lunine J. I., 1996, *Science*, 272
- Mazzitelli I., 1989, *ApJ*, 340, 249
- Meyer F., Meyer-Hofmeister E., 1999, *A&A*, 346, L13
- Meyer-Hofmeister E., Meyer F., Liu B. F., 1998, *A&A*, 339, 507
- Nelson L. A., Chau W. Y., Rosenblum A., 1985, *ApJ*, 299, 658
- Paczyński B., 1981, *Acta Astr.*, 31, 1
- Paczyński B., Sienkiewicz R., 1981, *ApJ*, 248, L27

- Patterson J., 1998, *PASP*, 110, 1132
Politano M., 1996, *ApJ*, 465, 338
Rappaport S., Joss P. C., Webbink R. F., 1982, *ApJ*, 254, 616
Ritter H., 1988, *A&A*, 202, 93
Ritter H., Kolb U., 1992, *A&A*, 259, 159
Ritter H., Kolb U., 1998, *A&A*, 129, 83
Saumon D., Chabrier G., Van Horn H. M., 1995, *ApJS*, 99, 713
Saumon D., Chabrier G., Wagner D. J., Xie X., 1998, *Phys. Rev.*,
submitted
Sills A., Pinsonneault M. H., 1999, *ApJ*, submitted (astro-ph/9903116)
- Stehle R., Ritter H., Kolb U., 1996, *MNRAS*, 279, 581
Stehle R., Kolb U., Ritter H., 1997, *A&A*, 320, 136
Uryu K., Eriguchi Y., 1999, *MNRAS*, 303, 329
Warner B., 1995, *Cataclysmic Variable Stars*, Cambridge Astrophysics Ser.
28, Cambridge Univ. Press, Cambridge
Watson M. G., 1999, in Hellier C., Mukai K., eds, *ASP Conf. Ser. Vol. 197*,
Annapolis Workshop on Magnetic Cataclysmic Variables, p. 291
Wynn G., Leach R., 1999, *MNRAS*, submitted

This paper has been typeset from a \TeX/L\AA\TeX file prepared by the author.